Nomenclature

All units are in SI

F	Thrust
v_e	Exhaust gases velocity
$\dot{m}$	Mass flow
I_t	Total Impulse
t	Time
g	Acceleration of gravity
g_0	Acceleration of gravity at sea level
ρ	Density
u	Velocity component in the first plane
v	Velocity component in the second plane
w	Velocity component in the third plane
γ	Specific heat ratio
R	Universal gas constant
Ri	Specific gas constant
$\dot{r}$	Regression rate
G	Free stream propellant mass velocity
μ	Viscosity coefficient
β	Blowing parameter
x	Direction tangential to the first plane
y	Direction tangential to the second plane
z	Direction tangential to the third plane
A	Frequency factor
E_a	Activation energy
T	Temperature
T_0	Static temperature
P	Pressure
P_0	Static pressure
P_e	Escape gas pressure
P_a	Ambient pressure
e	Total energy in control volume
h	Enthalpy
λ	Velocity component in the direction of the main gas flow
σ	Courant number
M_a	Mach number

Chapter I

1.1 Introduction

Rocket engine development history and space exploration history have always been tied so closely that one subject could not be treated without involving the other.

Space exploration is only possible because of rocket engines, in particular, chemical rockets.

Although there are many types of rockets, this work will only mention chemical rockets.

Rockets, just like Jet engines, are reaction engines. They create work by expelling matter at high speeds. The thrust they create is equal to the force by which the matter is expelled.

Unlike jet engines, chemical rockets carry both oxidizer and fuel that are required to produce a steady combustion process. Exhaust gases are accelerated to high speeds by converting the chemical energy of a reaction (between the fuel and oxidizer) into heat, which increases the temperate of exhaust gases, and then converting the heat into kinetic energy with the use of a convergent-divergent section, through which gases are forced to pass.

Due to the unique combination of acceptable levels of thrust, specific impulse and environmental safety, chemical rockets are still today the only feasible method of putting cargo and passengers in space.

Chemical rockets can be divided into three types:

1. Solid
2. Liquid
3. Hybrid

Solid rocket engines carry the fuel and oxidizer mixed and in the solid phased. The place where the propellant mixture is stored acts as “fuel” tank, as well as combustion chamber.

The combustion process is started with the use of an igniter to heat a small part of the mixture to a critical temperature. As combustion occurs, the flow of hot burned fuel will ignite the rest of the mixture.

Different geometries of solid fuel provide different thrust and specific impulse at given time intervals of flight.

The solid rocket engine presents various advantages, mainly:

1. Less complexity
2. Easily storable fuels

These two advantages imply reduced costs in development, production and operation.

One serious problem with solid rocket engines is the lack of capability to stop and restart combustion. Once ignition is done, the engine only stops working once all the fuel is used.

Liquid Rocket Engines carry fuel and oxidizer in separate tanks. Both are in their liquid phase.

The fuel and oxidizer are then injected into a combustion chamber through high pressure pumps. As long as both fuel and oxidizer are injected in the chamber, combustion will happen making the engine operational.

The liquid rocket engines present various advantages, mainly:

1. Higher efficiency
2. Stop/Restart/Throttle capabilities

The disadvantages are the excessive complexity added by the high pressure pumps and use of, generally, extremely low temperature liquids.

This has as main consequence higher costs in development, production and operation. Also, the extra complexity will necessarily increase the risk of failure due to more likely engineering errors in the development phase.

The *Hybrid Rocket Engines* present, in this context, a middle term solution. This type of engine stores fuel and oxidizer in different tanks. Either the fuel is in the liquid phase and the oxidizer is in the

solid phase or the fuel is in the solid phase and the oxidizer in the liquid phase, being the latest combination the most used.

Since the combination of solid fuel and liquid oxidizer is the one that will be studied in this thesis, this version will always be the one associated with hybrid rocket engines from hereafter.

As with the solid rocket engines, the tank that holds the fuel in the solid phase is where the combustion occurs and therefore it serves as a combustion chamber as well.

Similarly to the liquid rocket engine, the hybrid has stop/restart capability. Whenever the engine is required to stop working, the valve supplying the oxidizer into the fuel tank is closed. To restart combustion, the valve is simply opened again. Stop/restart capability is very important for manned space flights since it ensures a safe engine shut-down in case of malfunction.

The use of fuels in the solid phase presents an operational advantage over low temperature liquids. Operation and storage becomes simpler and costs are therefore reduced.

Joining both the main advantages of solid rocket engines and liquid rocket engines, the hybrid rocket engine presents itself as a very cost-effective solution for manned space flight.

Developing and building rocket engines is a very expensive activity. The costs associated with it have been the main reason behind the apparent slow progress of technology in this area.

However, the exact opposite has happened with computer technology, which has had since its begining an incredible advancement. It has reach a point where it can be used to significantly reduce development costs associated with rocket development through the use of computer simulations.

This thesis focus on a particular step of the development phase of a rocket:

- performance prediction

Development costs of rocket engines can be reduced by reducing the number of prototype testing in favour of numerical simulations.

Numerical simulations are therefore useful to reduce development costs of any type of rocket engine [7].

Hybrid rocket engines are the least used and well understood engine type of the three. With the turn of a new century and the increasing interest in hybrid rocket engines for manned space flight applications, related with space tourism, it is imperative that development methods become not only cheaper, but also faster.

This work's purpose is to develop a software structure in which future specific rocket engines can be theoretically studied after adding experimental data to the simulator's considerations.

1.2 Objectives

a) Initial development of a software tool that determines for hybrid rocket engines the theoretical:

1. Internal gas flows
2. Characteristics of combustion
3. Solid fuel regression rate
4. Engine performance

b) Using an existing small scale hybrid rocket engine geometry to continuously validate mathematical method as software development progresses.

Chapter II

2.1 Principles of Rockets

2.1.1 **In-Flight Forces**

During atmospheric powered flight there are three forces applied to rockets:

1. Weight
2. Drag
3. Thrust

Weight is only present as long as the rocket is under the gravitational pull of a nearby planet or object. Drag is caused by the existence of friction between the rocket and the surrounding atmosphere, in case it exists. And finally, thrust is the force created by the rocket engine and applied on the rocket.

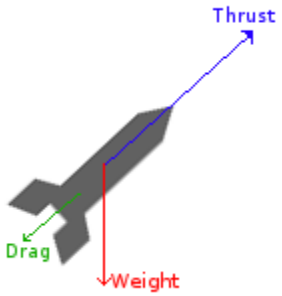

Fig. 1 – Forces applied a rocket during flight.

2.1.2 **Thrust**

On chemical rocket engines, chemical energy obtained from the combustion process is converted into kinetic energy which is used to accelerate the exhaust gases.

Thrust in a rocket, given by equation (1), is the reaction created by the force which is accelerating the exhaust gases out of the rocket nozzle.

$$F = \dot{m} * v_e - (P_e - P_a) * A_e \qquad (1)$$

2.1.3 **Impulse**

Total impulse, given by equation (2), is the thrust force integrated over time.

$$I_t = \int_0^t F\,dt \qquad (2)$$

If thrust is constant over a time interval dt, equation (3) gives the total impulse.

$$I_t = F * t \qquad (3)$$

Specific Impulse is the amount of time an engine can sustain a certain thrust. This is a very important parameter to know the performance of a rocket engine.

When thrust and mass flow vary over time, specific impulse relates to the thrust average over that time interval, as equation (4) shows:

$$I_s = \frac{\int_0^t F\,dt}{g\int_0^t mdot\,dt} \qquad (4)$$

In this case, the gravity pull is considered constant over the covered distance. Since the gravitational attraction between two bodies, in this case the rocket and the planet, is a function of the distance existing between them, the prediction has an error that increases with the increase in distance between the rocket and the planet.

For the present work, g will be assumed constant, since only the engine is being studied and not the actual flight of the rocket.

2.1.4 **Mass flow**

The total mass of a rocket is given by equation (5):

$$mass_{total} = mass_{rocket} + mass_{payload} + mass_{propellants} \quad (5)$$

For the scope of this work $mass_{rocket}$ and $mass_{payload}$ are not important.

In hybrid rockets $mass_{propellants}$ is equal to the mass of the oxidizer plus the mass of the fuel (equation 6), either is it a liquid-solid or solid-liquid combination, respectively.

$$mass_{propellants} = mass_{oxidizer} + mass_{fuel} \quad (6)$$

Therefore, mass flow coming out of the engine will be given by equation (7):

$$\dot{m} = v_e * \rho_{gas} * A_e \quad (7)$$

2.1.5 **Nozzle**

2.1.5.1 Ideal rocket

The ideal rocket concept consists of expressing complex thermodynamic principles as simple mathematical expressions. Even with simplifications, the actual performance of the rocket is usually only between 1% and 6% below the calculated ideal rocket performance [1].

The ideal rocket is one in which the following list of assumptions is valid:

1. *The working substance is homogeneous.*
2. *All the species of the working fluid are gaseous. Any condensed phases add a negligible amount of to the total mass.*
3. *The working substance obeys the perfect gas law.*
4. *There is no heat transfer across the rocket walls; therefore, the flow is adiabatic.*
5. *The is no appreciable friction and all boundary layer effects are neglected.*
6. *There are no shock wave or discontinuities in the nozzle flow.*

7. *The propellant flow is steady and constant. The expansion of the working fluid is steady and constant, without vibration. Transient effects are of very short duration and may be neglected.*
8. *All exhaust gases leaving the rocket have an axially directed velocity.*
9. *The gas velocity, pressure, temperature, and density are all uniform across any section normal to the nozzle axis.*
10. *Chemical equilibrium is established within the rocket chamber and the gas composition does not change in the nozzle (frozen flow).*
11. *Stored propellants are at room temperature. Cryogenic propellants are at their boiling points. [1]*

2.1.5.2 Nozzle De Laval

The Nozzle De Laval is a bell-shaped convergent-divergent section of the rocket engine (fig. 2 [below]).

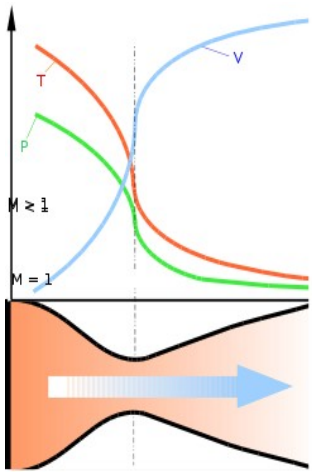

Fig. 2 – Temperature, pressure and gas velocity variation in the nozzle (above) and nozzle DeLaval (below). Image source: Wikimedia Commons

Its purpose is to convert heat into kinetic energy.

The gas flow is forced to accelerate to Mach speed from the interior to the nozzle throat, thus making the gas lose temperature and pressure (fig. 2 [above]).

The divergent section further allows the gas flow to accelerate while redirecting it in opposite direction to the rocket's heading.

2.1.5.3 Optimal,Under- and over- expanded nozzles

The difference between escape gas pressure and external pressure has an important effect on overall engine performance, as shown by equation (1).

A nozzle in which the escape gas pressure is equal to the external pressure is said to have an optimal expansion. If the escape gas pressure is lower than the external pressure, the nozzle is said to be under-expanded. On the other hand, if the escape gas pressure is higher than the external gas pressure, the nozzle is over-expanded.

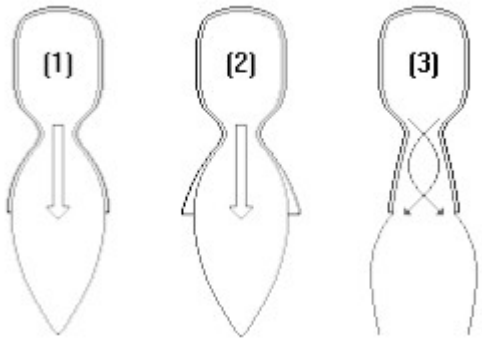

Fig. 3 – (1) Optimal expansion; (2) Under-expanded; (3) Over-expanded.

For optimal expansion nozzles, the total thrust is given by equation (8):

$$F = \dot{m} * v_e \qquad (8)$$

Rockets usually have different nozzle geometries in every stage, each of which are optimized for the pressure of the intended operational altitude.

2.1.5.4 Escape velocity

The escape gas velocity of a rocket engine can be estimated with equation (9):

$$v_e = \sqrt{\frac{2k}{k-1} R T_1 \left[1 - \left(\frac{p_e}{p_1}\right)^{\frac{(k-1)}{k}}\right] + v_1^2} \qquad (9)$$

where:

p_1 is the nozzle inlet gas pressure,
p_e is the escape gas pressure,
T_1 is the nozzle inlet gas temperature,
k is the specific heat ratio of the mixture, and
v_1 is the nozzle inlet gas velocity.

This equation is valid as long as the rocket is considered to be ideal.

2.2 The Hybrid Rocket Engine

2.2.1 **Overview**

A Hybrid rocket engine is one in which one of the propellants is in its solid phase and the other is in its liquid phase (fig. 4).

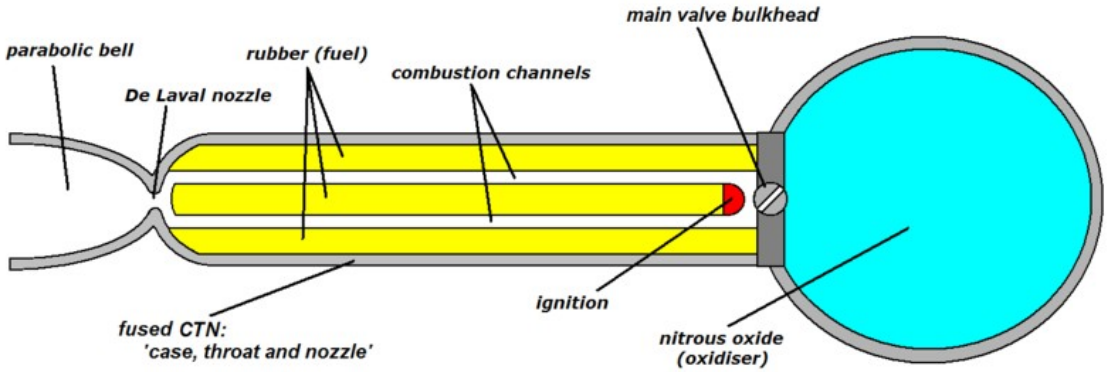

Fig. 4 – Hybrid rocket engine of Spaceshipone. Courtesy of ScaledComposites.

Usually the oxidizer is in its liquid phase and the fuel is in the solid phase.

As with solid rocket engines, the geometry of the solid fuel determines the thrust curves of the hybrid. With an increase in contact area between the hot gas flow and the solid fuel surface, thrust originated by the engine will increase, since more mass is reacting.

Although hybrid engines are safer than solid rocket engines, they suffer from some of the same problems. A large enough crack in the solid fuel will lead to an unexpected increase in chamber pressure that may result in a catastrophic failure.

Unlike liquid rocket engines, the flow of oxidizer in hybrids won't provide a near stoichiometric combustion process. This causes some parts of the fuel wall to regress faster than others, leading to an increasingly unpredictable resultant thrust. This is the main reason why hybrid engines aren't chosen for military applications.

The geometry of a typical hybrid is cylindrical (fig. 5) with a hole in the middle to allow gas flow and contact of the oxidizer with the solid fuel. Usually, engines have an empty space before and after the solid fuel to allow gas recirculation. The recirculation of flow will allow some of the un-burnt fuel and oxidizer to react before exiting the chamber, thus increasing the efficiency of the propulsion system.

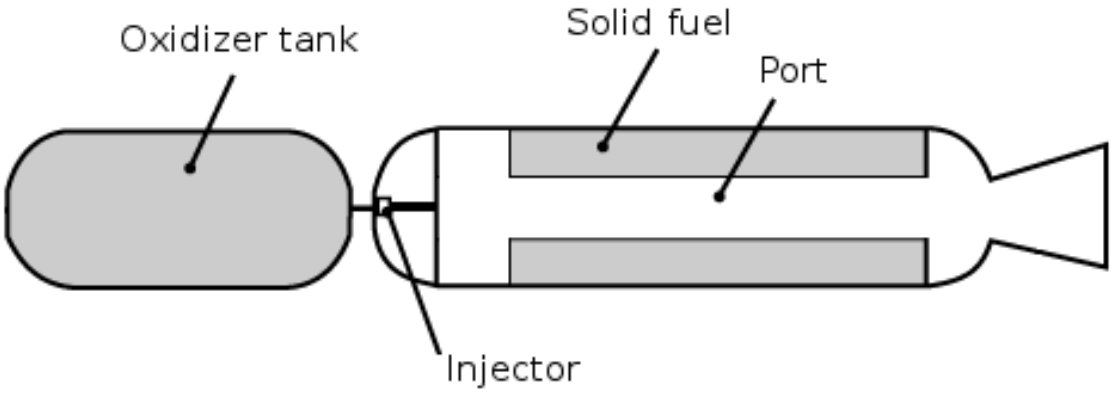

Fig. 5 – Conventional hybrid rocket engine.

As soon as the first reactions occur, a turbulent flow is created. The resultant hot gas is transported through that turbulence within the boundary layer (also known as “force convection” [14]).

The heat originated by the reaction gradually liquefies and then gasifies or directly sublimates the solid fuel surface. It is also common that small bits of solid fuel are released without changing phase and therefore not reacting. Poorly designed engines may explode because large parts of solid fuel are released and end up blocking the chamber's exit.

There is a vaporized fuel rich zone in the layer immediately above the solid fuel surface (fig. 6). This section exists because of the heat released from the flame zone layer above it, where reactions occur.

In the flame zone, the mixture of fuel and oxidizer is virtually stoichiometric. The heat released will also help vaporize the entering oxidizer, further increasing the completeness of the reactions and thus improving engine performance.

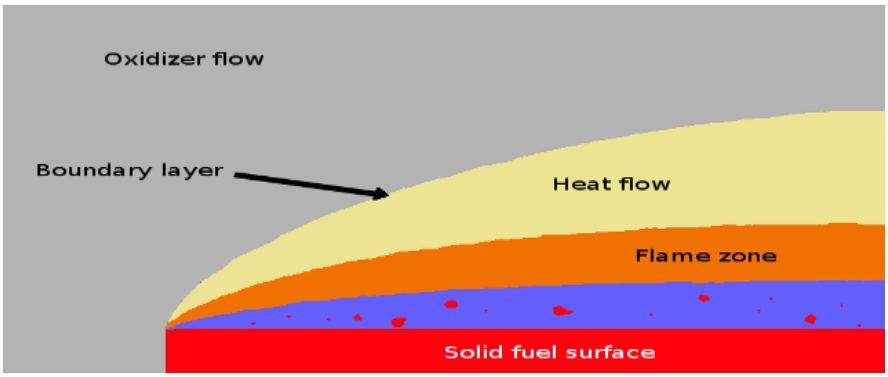

Fig. 6 – Different zones of mixture properties.

2.2.2 **Regression rate**

Regression rate ($\dot{r}$) is the length of solid fuel volume that is burned in a chosen time-step.

The increase of $\dot{r}$ is normally associated with an increase in thrust output, since higher $\dot{r}$ implies that a larger solid fuel surface will be exposed to the gas flow, thus increasing the number of chemical reactions.

Equation (10) is an *Arrhenius* derived formula that determines an approximate value of $\dot{r}$ at a given axial location x:

$$\dot{r} = 0.036 \frac{G^{(0.8)}}{\rho_f} \left(\frac{\mu}{x}\right)^{(0.2)} B^{(0.23)} \qquad (10)$$

where:

G is the free stream propellant mass velocity,
ρ_f is the density of the solid fuel,
μ is combustion gas viscosity, and
β is the non-dimensionalized fuel mass flux (normally refered to as *blowing parameter*).

As we can see from equation (10), unlike solid rocket engines where $\dot{r}$ is mainly dependent of the combustion chamber pressure, in hybrids, $\dot{r}$ is highly dependent of the free stream propellant mass velocity.

2.3 Aspire-Space H2 Rocket Engine

Hybrid rocket engines have seen a lot of development in the United Kingdom at the hands of amateur rocketeers. Thanks to their efforts and enthusiasm, much interest has now been taken on hybrid engines.

Solid rocket engines are the amateur rocketeers' favourite engine due to its simplicity and ease of launch. However, due to a UK law that forbids the use of solid fuels by civilians, because of their instability, the communities have turned their attentions on the hybrid configuration. Propellants used in Hybrid rockets are more easily obtained, stored and used, when comparing to the ones of liquid rocket engines.

Aspire-space was a group of amateur rocketeers that developed solid engines and later moved to the development of hybrid engines.

H2 is one of those engines (fig. 7):

Fig. 7 – Aspirespace's H2 engine during a static test-fire.
Courtesy of Aspirespace.

This engine uses nitrous oxide as oxidizer and high-density polyethelene (HPDE) as fuel.

The engine's fuel geometry is conventional. A cylindrical solid fuel geometry with a cylindrical port. A post-combustion section exists to allow flow recirculation (fig. 8).

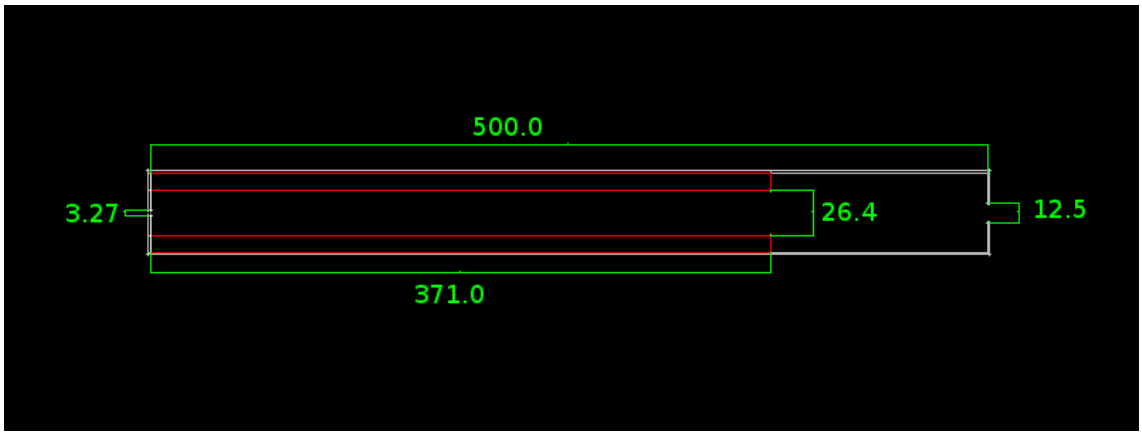

Fig. 8 – 2D approximate scheme of the H2 engine. Injection of the left, chamber exit on the right. White lines represent the chamber casing. Red lines represent the solid fuel geometry. Units in millimetres.

The H2 was completed in 1998 and tested in May of that year. Since then, the H2 has been successfully test fired various times, allowing for a lot of information about its performance to be gathered. ADV rockets use this type of engine.

There are three planned rockets from de ADV series, ADVa, ADVb and ADVc. ADVb is an improved version of ADVa, while ADVc is ADVb's upper stage.

ADVb simulation predicted the capability of reaching 24000 feet above launch pad.

ADVc (fig. 9) was test launched on the Highlands of Scotland. Performance was below expected because of a nitrous oxide leak before take-off, which radically reduced the tank pressure [20].

Fig. 9 – Aspirespace ADVc. Courtesy of Aspirespace.

2.4 Combustion Process

2.4.1 **Chemical reaction**

The chemical reaction that occurs within the chamber of the H2 between the nitrous oxide and the HPDE can be described by equation 11:

$$N_2O + C_2H_4 + (5/2)\ O_2 \longrightarrow 2\ N + 2\ H_20 + 2\ C0_2 \qquad (11)$$

1 mol of nitrous oxide (N_2O),
1 mol of High-Density Polyethelene (C_2H_4) and
5/2 mols of oxygen ($(5/2)\ O_2$) ,

Have a stoichiometric reaction giving place to:

2 mols of Nitrogen (2 N),
2 mols of Water ($2\ H_20$) and
2 mols of Carbon Dioxide ($2\ C0_2$).

2.4.2 **Reaction rate equation**

2.4.2.1 Reaction rate

The rate of change of quantities of elements in a given reaction can be approximately calculated with equation (12):

$$rate = k \,.\, [A]^a \,.\, [B]^b \qquad (12)$$

where:

rate is the rate of change of elements given in [mol . dm^{-3} s^{-1}],
k is a called the rate constant,
[A] and [B] are concentrations of elements A and B respectively given in mol dm^{-3},
a and *b* are the orders of reaction.

2.4.2.2 Orders of reaction

Order of reaction is the power the concentration of an element has in influencing the reaction rate of a reaction process in which that element is involved in. It is a dimensionless coefficient.

Orders of reaction can only be determined through analysis of practical data.

2.4.2.3 Arrhenius equation

Although *k* is called the “rate constant”, the name is in fact misleading since *k* depends of various factors and varies with *temperature*, *activation energy* and with the *frequency factor*, which is also dependent of several other gas properties.

k can be calculated using an equation determined by Svante Arrhenius (13):

$$k = A e^{\left(\frac{-E_a}{RT}\right)} \qquad (13)$$

where:

A is the frequency factor,
E_a is the reaction's activation energy,

e is the Nepper constant number which is approximately equal to 2.71828,
R is the universal gas constant, and
T is the temperature.

2.4.2.4 Frequency factor

This variable is a function of the frequency of collisions and their orientation. Although it varies slightly with the variation of temperature, it can be considered constant over small intervals of temperature.

2.4.2.5 Activation energy

For a reaction to occur, the gas has to have a certain amount of energy. That energy is called activation energy. The rate of reaction is a function of this variable.

Lower activation energy means higher reaction rate.

2.5 Fluid Mechanics

2.5.1 **Navier-Stokes Equation**

In fluid mechanics, the equations that describe a fluid's motion are the Navier-Stokes equations (14).

$$\rho\left(\frac{\partial u}{\partial t}+u\frac{\partial u}{\partial x}+v\frac{\partial u}{\partial y}+w\frac{\partial u}{\partial z}\right)=-\frac{\partial P}{\partial x}+\mu\left(\frac{\partial^2 u}{\partial x^2}+\frac{\partial^2 u}{\partial y^2}+\frac{\partial^2 u}{\partial z^2}\right)$$
$$\rho\left(\frac{\partial v}{\partial t}+u\frac{\partial v}{\partial x}+v\frac{\partial v}{\partial y}+w\frac{\partial v}{\partial z}\right)=-\frac{\partial P}{\partial y}+\mu\left(\frac{\partial^2 v}{\partial x^2}+\frac{\partial^2 v}{\partial y^2}+\frac{\partial^2 v}{\partial z^2}\right)$$
$$\rho\left(\frac{\partial w}{\partial t}+u\frac{\partial w}{\partial x}+v\frac{\partial w}{\partial y}+w\frac{\partial w}{\partial z}\right)=-\frac{\partial P}{\partial z}+\mu\left(\frac{\partial^2 w}{\partial x^2}+\frac{\partial^2 w}{\partial y^2}+\frac{\partial^2 w}{\partial z^2}\right)$$

Eq. (14) – Momentum conservation.

These equations consider a infinitesimal volume, usually called control volume.

In computational fluid mechanics, there are three categories of considerations' simplification for flow calculation using the Navier-Stokes equations. They are:

1. *Gas dynamics* – compressible frictionless flows
2. *Viscous flows, boundary layers and turbulence* – Incompressible frictional flows
3. *Potential frictionless flows*

The present study will take in consideration just the first category because of the following reasons:

1. *A high Reynolds number is expected for the gas flow within the chambe*r – Inertial forces are expected to largely surpass viscous forces, which can therefore be neglected
2. *Compressibility is expected to play a significant role in achieving a more accurate perspective of gas flows and also a more accurate combustion process calculation*

The compressible, frictionless form of the Navier-Stokes equations is usually refered to as Euler equations.

2.5.2 **Euler Equations**

Euler equations are a special case of the Navier-Stokes equations. Since viscosity is considered negligible, μ becomes 0. Equations (15) are the differential form of the Euler equations.

$$\frac{\partial \rho}{\partial t}+\frac{\partial \rho u}{\partial x}+\frac{\partial \rho v}{\partial y}+\frac{\partial \rho w}{\partial z}=0$$

$$\frac{\partial \rho u}{\partial t}+\frac{\partial \rho u^2+P}{\partial x}+\frac{\partial \rho vu}{\partial y}+\frac{\partial \rho wu}{\partial z}=0$$

$$\frac{\partial \rho u}{\partial t}+\frac{\partial \rho uv}{\partial x}+\frac{\partial \rho v^2+P}{\partial y}+\frac{\partial \rho wv}{\partial z}=0$$

$$\frac{\partial \rho u}{\partial t}+\frac{\partial \rho uw}{\partial x}+\frac{\partial \rho vw}{\partial y}+\frac{\partial \rho w^2+P}{\partial z}=0$$

Eq. 15 – Euler system of equations in their differential form.

2.6 Gas Dynamics Computational Method

2.6.1 **Control volumes' grid**

For a three-dimensional grid of control volumes, using the Cartesian coordinates, the configuration is as follows (Fig. 10):

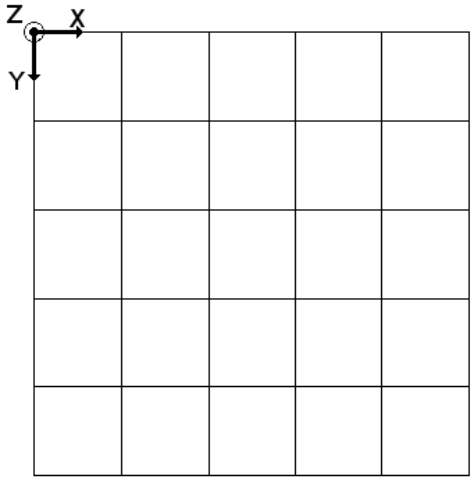

Fig. 10 – Control volume grid representation based on Cartesian coordinates

For cylindrical coordinates (Fig. 11):

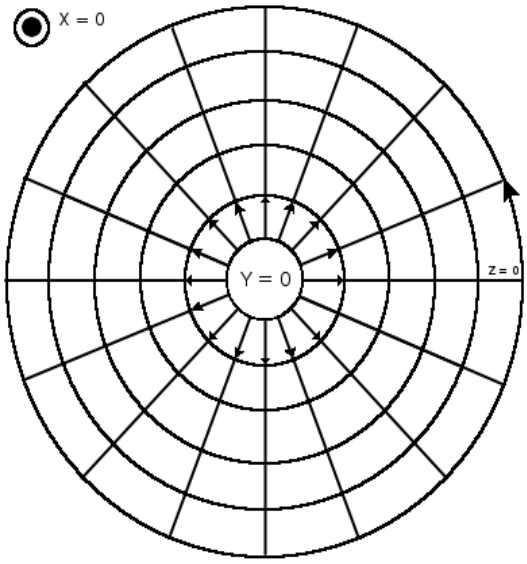

Fig. 11 – Control volume grid representation based on cylindrical coordinates

2.6.2 **Time-Marching method applied to Euler equations**

Time-marching methodology consists of solving a given equation, or set of equations, for a defined progressive quantity step.

Considering, for example, equations (16) and (17):

$$y' = f(x, y) \qquad (16)$$
$$y(x_0)\ ) = y_0 \qquad (17)$$

Having the solution for an initial value, such as the one given by equation (17), and if the solution varies with a certain quantity step h, it is possible to solve the following system of equations (18):

$$y\ (x + h) = y(x) + h[f(x, y)]$$
$$y'(x) = [y(x + h) - y(x)] / h \qquad (18)$$

Now, applying to the Euler system of equations (19):

$$\delta\rho^{[t+1]} = \delta\rho^{t} + \frac{\delta\rho}{\delta t}$$

$$\delta\rho u^{[t+1]} = \delta\rho u^{t} + \frac{\delta\rho u}{\delta t}$$

$$\delta\rho v^{[t+1]} = \delta\rho v^{t} + \frac{\delta\rho v}{\delta t}$$

$$\delta\rho z^{[t+1]} = \delta\rho z^{t} + \frac{\delta\rho z}{\delta t}$$

$$\delta\rho e^{[t+1]} = \delta\rho e^{t} + \frac{\delta\rho e}{\delta t}$$

(19)

To programme the time-marching method applied to the Euler equations it is first necessary to discrete-size the system. Considering the Cartesian system of coordinates indicated on fig. 10, the three-dimensional discrete form of the equations is as follows (20):

$$\rho^{t+1} = \rho^{t} + \{ (\Delta y)*(\Delta z)*[(\rho u)_{left} - (\rho u)_{right}]^t + (\Delta x)*(\Delta z)*[(\rho v)_{above} - (\rho v)_{below}]^t + (\Delta x)*(\Delta y)*[(\rho z)_{front} - (\rho z)_{back}]^t \}*(\Delta t/\Delta V)$$

$$\rho u^{t+1} = \rho u^{t} + \{ (\Delta y)*(\Delta z)*[(\rho*u^2 + P)_{left} - (\rho*u^2 + P)_{right}]^t + (\Delta x)*(\Delta z)*[(\rho*v*u)_{above} - (\rho*v*u)_{below}]^t + (\Delta x)*(\Delta y)*[(\rho*z*u)_{front} - (\rho*z*u)_{back}]^t \}*(\Delta t/\Delta V)$$

$$\rho v^{t+1} = \rho v^{t} + \{ (\Delta y)*(\Delta z)*[(\rho*u*v)_{left} - (\rho*u*v)_{right}]^t + (\Delta x)*(\Delta z)*[(\rho*v^2 + P)_{above} - (\rho*v^2 + P)_{below}]^t + (\Delta x)*(\Delta y)*[(\rho*z*v)_{front} - (\rho*z*v)_{back}]^t \}*(\Delta t/\Delta V)$$

$$\rho z^{t+1} = \rho z^{t} + \{ (\Delta y)*(\Delta z)*[(\rho*u*z)_{left} - (\rho*u*z)_{right}]^t + (\Delta x)*(\Delta z)*[(\rho*v*z)_{above} - (\rho*v*z)_{below}]^t + (\Delta x)*(\Delta y)*[(\rho*z^2 + P)_{front} - (\rho*z^2 + P)_{back}]^t \}*(\Delta t/\Delta V)$$

$$\rho e^{t+1} = \rho e^{t} + \{ (\Delta y)*(\Delta z)*[(\rho*u*h)_{left} - (\rho u*h)_{right}]^t + (\Delta x)*(\Delta z)*[(\rho*v*h)_{above} - (\rho*v*h)_{below}]^t + (\Delta x)*(\Delta y)*[(\rho*z*h)_{front} - (\rho*z*h)_{back}]^t \}*(\Delta t/\Delta V)$$

(20)

To apply this system to a cylindrical coordinates system, the following considerations are used:

Cylinder length ⇔ X coordinate
Radius ⇔ Y coordinate :
1. Radius – 1 ⇔ Above
2. Radius + 1 ⇔ Below

Angle ⇔ Z coordinate :
1. Angle – 1 ⇔ Front
2. Angle + 1 ⇔ Below

2.6.3 **Courant-Friedrichs-Lewy condition**

In order to apply the Euler equations for each cell of a grid of control volumes, it is of critical importance that we know, at each time-step, the exact conserved quantities in each one of the cells. Choosing to ignore such fact would lead to excessively complex programming in order to prevent loss of information while attempting to solve the equations.

The Courant-Friedrichs-Lewy condition, hereafter refered to as CFL, allows us to determine a time-step value that ensures the programmer that per each time-step, the conserved quantities of each cell will only be dislocated to their immediate neighbour.

The result of the following equation (21) is called the Courant number:

$$\sigma = \lambda * \Delta t / \Delta x \qquad (21)$$

where:
λ is the velocity of the mass flow in the x direction,
Δt is the time-step,
Δx is the length of the control volume is the x direction.

To determine a time-step that will prevent loss of information while solving the Euler equations, the following condition must be established (equation 22):

$$\sigma < 1 \qquad (22)$$

Thus, the maximum time-step allowed to use in the solver would be given by equation (23):

$$\Delta t < \Delta x / \lambda \qquad (23)$$

Special care must be taken when considering a three-dimensional solver. Considering the x,y and z dimensions, and being the length of each dimension given by equation (24):

$$\Delta y < \Delta x < \Delta z \qquad (24)$$

The maximum time-step that can be used is given by equation (25):

$$\Delta maximum = \Delta y / \lambda_y < \Delta x / \lambda_x < \Delta z / \lambda_z \qquad (25)$$

In his book, the author M. Lobo [8] calculates for each control volume an individual time-step. This allows him to save memory space and reduce the number of calculations to the minimum required.

Considering today's incredible computer power, such care for this type of applications is not required any more.

2.6.4 **Wall boundary condition**

Determining the change in conserved quantities at each control volume always requires the values of the conserved quantities of its neighbouring cells. So when a control volume is near a wall, special considerations must be made.

The Euler equations consider the fluid inviscid, so at the limit of a fluid near a wall, there will only be a tangential velocity component. This is called the *slip condition* (Fig. 12).

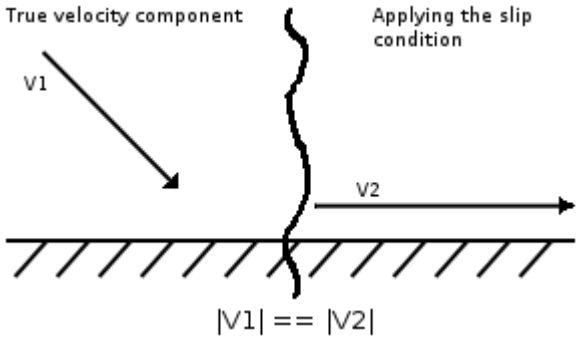

Fig. 12 – Slip condition

Since a wall is present, and considering it to be impermeable, obviously there can not be any fluid velocity vector perpendicular to to the wall and in its direction. So, near a wall, the normal velocity vector with direction towards it will always be zero.

However, by deleting a vector component of velocity, we'll be removing a certain amount of energy given by equation (26):

$$\textit{removed energy} = 0.5*(\text{velocity vector element})^2 \qquad (26)$$

This would necessarily cause a violation in the energy-momentum conservation.

To minimize this event, it is commonly used in the literature [8, 9] the method of adding the deleted velocity component to the other velocity components that are not pointing toward any wall boundaries.

2.6.5 **Inlet boundary condition**

For control volumes near the chamber inlet (also called injector, in the case of rocket engines), special boundary conditions must be considered since additional fluid in entering the grid.

The approach recommended by Lobo [8] consists of defining initial values of flow Mach number, static pressure and static temperature for the entry fluid.

Temperature is then calculated using equation (27):

$$T = \frac{T_0}{1 + 0.5(\gamma - 1)\,Ma^2} \qquad (27)$$

After determining the local speed of sound, considering the gas mixture properties, the entry velocity can be calculated using equation (28):

$$\text{Entry velocity} = \text{Local Mach number} * \text{Local speed of sound} \qquad (28)$$

Pressure is calculated with equation (29):

$$P = P_0 \left(\frac{1}{(1 + 0.5(\gamma - 1)\,Ma^2)} \right)^{\left(\frac{\gamma}{\gamma - 1}\right)} \qquad (29)$$

Density is calculated with the perfect gas law (30):

$$\rho = \frac{P}{R_i T} \qquad (30)$$

We now have all the required parameters to construct boundary conditions for the first control volumes near the grid's gas entry.

2.6.6 **Outlet boundary condition**

Outlet boundary conditions (near the exit of the combustion chamber) can be determined by making an extrapolation from the interior.

Lobo [8] does the following extrapolation (equations 31, 32, 33, 34, 35):

$$\rho_{outlet} = 2 * \rho_{outlet-2\,cells} - \rho_{outlet-1\,cell} \quad (31)$$

$$P_{outlet} = 2 * P_{outlet-2\,cells} - P_{outlet-1\,cell} \quad (32)$$

$$Vx_{outlet} = 2 * Vx_{outlet-2\,cells} - Vx_{outlet-1\,cell} \quad (33)$$

$$Vy_{outlet} = 2 * Vy_{outlet-2\,cells} - Vy_{outlet-1\,cell} \quad (34)$$

$$Vz_{outlet} = 2 * Vz_{outlet-2\,cells} - Vz_{outlet-1\,cell} \quad (35)$$

Using the perfect gas law, the temperature of the exiting gas can be determined (36):

$$T_{outlet} = \frac{P_{outlet}}{R_i \rho_{outlet}} \quad (36)$$

We now have all the required parameters to construct boundary conditions for the last control volumes near the grid's gas exit.

2.6.7 **Artificial dissipation**

Artificial dissipation, also known as *artificial viscosity,* is a mathematical solution to prevent numerical error driven oscillations from increasing with each time-step as Euler equations are solved.

Although the term *viscosity* is used, the mathematical solution has no direct physical connection with that particular property of the fluid.

The usual criteria for stability are strictly valid only for linear equations. Non-linear equations will generally have solutions that are difficult to pursue rigorously. Attempting such a pursuit would eventually lead to divergent solutions without any physical meaning.
To prevent this, authors have developed mathematical methods simply used to stabilize the solving algorithm.

The concept of artificial viscosity (more correctly called artificial dissipation) was first introduced by Von Neumann and R. D. Richtmyer during the WWII, but since the study was classified. It was only released after the war [9].

Applying artificial viscosity to the time-marching method using Euler equations consists in adding an additional member to the left part of the equations (37):

$$\delta\rho^{[t+1]} = \delta\rho^{t} + \frac{\delta\rho}{\delta t} + A\rho$$

$$\delta\rho u^{[t+1]} = \delta\rho u^{t} + \frac{\delta\rho u}{\delta t} + A\rho u$$

$$\delta\rho v^{[t+1]} = \delta\rho v^{t} + \frac{\delta\rho v}{\delta t} + A\rho v$$

$$\delta\rho z^{[t+1]} = \delta\rho z^{t} + \frac{\delta\rho z}{\delta t} + A\rho z$$

$$\delta\rho e^{[t+1]} = \delta\rho e^{t} + \frac{\delta\rho e}{\delta t} + A\rho e$$

(37)

where $A\rho$, $A\rho u$, $A\rho v$, $A\rho z$ and $A\rho e$ are numerical stabilizers for the solver algorithm.

In his book, Lobo [8] presents the following pratical form of applying artificial dissipation to a 2D solver:

f in the following equation (38) refers to any of the conserved quantities, ρ, ρv_x, ρv_y and ρe.

$$Af = a^{+}_{x1} f^{+}_{x1} - a^{-}_{x1} f^{-}_{x1} - a^{+}_{x3} f^{+}_{x3} - a^{-}_{x3} f^{-}_{x3} + a^{+}_{y1} f^{+}_{y1} - a^{-}_{y1} f^{-}_{y1} - a^{+}_{y3} f^{+}_{y3} - a^{-}_{y3} f^{-}_{y3} \quad (38)$$

where - and + superscripts indicate the neighbouring cell closest to 0 coordinate and the neighbouring cell on the oposite side, respectively.

The terms used to define *Af* are given by equations (39 to 54):

$$a^{+}_{x1}=a_1 max[p_{xx}(i,j), p_{xx}(i+1,j)] \quad (39)$$

$$a^{-}_{x1}=a_1 max[p_{xx}(i,j), p_{xx}(i-1,j)] \quad (40)$$

$$a^{+}_{y1}=a_1 max[p_{yy}(i,j), p_{yy}(i,j+1)] \quad (41)$$

$$a^{-}_{y1}=a_1 max[p_{yy}(i,j), p_{yy}(i,j-1)] \quad (42)$$

$$a^{+}_{x3}=max[(a_3-a^{+}_{x1}),0] \quad (43)$$

$$a^{-}_{x3}=max[(a_3-a^{-}_{x1}),0] \quad (44)$$

$$a^{+}_{y3}=max[(a_3-a^{+}_{y1}),0] \quad (45)$$

$$a^{-}_{y3}=max[(a_3-a^{-}_{y1}),0] \quad (46)$$

$$f^{+}_{x1}=f(i+1,j)-f(i,j) \quad (47)$$

$$f^{-}_{x1}=f(i,j)-f(i-1,j) \quad (48)$$

$$f^{+}_{x3}=f(i+2,j)-3f(i+1,j)+3f(i,j)-f(i-1,j) \quad (49)$$

$$f^{-}_{x3}=f(i+1,j)-3f(i,j)+3f(i-1,j)-f(i-2,j) \quad (50)$$

$$f^{+}_{y1}=f(i,j+1)-f(i,j) \quad (51)$$

$$f^{-}_{y1}=f(i,j)-f(i,j-1) \quad (52)$$

$$f^{+}_{y3}=f(i,j+2)-3f(i,j+1)+3f(i,j)-f(i,j-1) \quad (53)$$

$$f^{-}_{y3}=f(i,j+1)-3f(i,j)+3f(i,j-1)-f(i,j-2) \quad (54)$$

where:

$$p_{xx}=\frac{P(i+1,j)-2P(i,j)+P(i-1,j)}{P(i+1,j)+2P(i,j)+P(i-1,j)} \quad (55)$$

$$p_{yy} = \frac{P(i, j+1) - 2P(i, j) + P(i, j-1)}{P(i, j+1) + 2P(i, j) + P(i, j-1)} \qquad (56)$$

a_1 and a_3 are coefficients that need to defined by the programmer. The higher their value, less physical meaning will the solution of the Euler equations have.

2.7 State of the Art

2.7.1 Numerical Simulations on Hybrid Rocket Engines

Unlike Solid Rocket Engines that have been well studied over the years, few relevant papers exist on Hybrids.

The work of authors Guobiao C. and Hui T. from the Beijing University of Aeronautics and Astronautics [11] closely resembles the objectives presented in this thesis.

In their work, the authors studied the theoretical propellant performance, solid fuel regression rate, characteristics of combustion and gas flow of a classical hybrid rocket engine.

The oxidizer/fuel combination studied was Liquid Oxygen and HTPB.

To estimate the solid fuel regression rate, the authors used an formula derived from equation (10). This allowed them to calculate the regression rate at different axial distances from the oxidizer injection, as a function of that same distance and also of the total oxidizer mass velocity.

From this estimate, the authors concluded that the average regression rate increases with the increase of total oxidizer mass flow and/or grain length *.

As expected, an increase of total oxidizer mass and/or grain length also resulted in an increase in adiabatic combustion temperature, since higher availability of oxidizer has as consequence more exothermic reactions.

The authors also calculated the nozzle flow using the axial symmetry, unsteady, compressible, non-equilibrium, turbulent, Reynolds average Navier-Stokes equations. Force and thermal radiation were ignored.

Computed temperature on the nozzle is higher near the walls and lower near the central axis.

The authors also showed that thrust control on a hybrid can be easily achieved by simply changing the oxidizer mass flow.

* - Grain length is the length of port which has solid fuel.

2.7.2 **Existing software**

Various numerical simulators exist on the web that allow to estimate an average hybrid engine performance. The performance output parameters are usually thrust, solid regression rate and specific impulse, given by equations 4, 1 and 10, respectively. These simple programs are usually Javascript applications for use by amateur rocketeers.

Although simple, these applications provide sufficiently accurate results for an initial performance prediction of small rockets.

Still, these applications cannot provide an insight into to the engine's gas dynamics and combustion process.

There are some complex commercial computational dynamics software, such as Fluent, that can be applied to hybrid rocket engines providing professional level theoretical results. This kind of software is expensive and is usually out of the reach of common rocketry enthusiasts and teaching institutions such as colleges or in some cases, universities.

Chapter III

3.1 Mathematical Model

3.1.1 **Gas flow solver**

The method used to determine the gas flow motion within the combustion chamber is based on the inviscid *Navier-Stokes* equations (*Euler equations*). Mass conservation, momentum and energy equations are calculated. Two-dimensional and three-dimensional versions of the solver were attempted.

Due to problems with boundary conditions, two-dimensions were first used instead of three-dimensions, although source code was left ready for quick re-implementation of three-dimensions.

After attempting the use of Cartesian coordinates system, a Cylindrical coordinates system was instead chosen because of limitations of the first.

The combustion chamber space is divided into various control volumes. For each of these volumes, the Euler equations are calculated in order to know the density, gas velocity field and energy variations.

Time-Marching is used to progressively calculate the moving quantities.

All the fluid in motion within the chamber is considerer to be in its gaseous phase. This includes the oxidizer, as soon as it exits the oxidizer tank, as well as the fuel, as soon as it seperated from the solid fuel surface.

The fluid is considerer a perfect gas, and therefore the perfect gas equation is used to establish a relationship between pressure, density and temperature.

With the exception of the engine's injector, solid fuel surface and chamber exit, no density, energy or momentum is loss or gained through the chamber walls.

Inlet border conditions enunciated in section 2.6.6 are used for both oxidizer entry and fuel entry.

Outlet border conditions enunciated in section 2.6.7 are used for the chamber exit.

Slip condition is applied on the chamber walls.

The established time-step is set following the *CFL condition*. A single time-step is used for the whole grid. This allows the flow solver to be synchronized with the equations related with the chemical reaction process.

The use of artificial dissipation was initially used, but eventually removed due to its evident negative effect on data validity. It is a requirement of HESS to know for each control volume the gas mixture properties, as well as the density flow. Artificial dissipation would desynchronise the gas flow solver and the combustion process solver.

3.1.2 **Combustion process solver**

3.1.2.1 Artificial sublimation

Solid fuel is sublimated and added to the gas flow through the walls of the control volumes near the solid fuel surface.

The rate of entry is calculated with the empirical equation (57), which determines a Mach entry value to use in the boundary conditions enunciated in section 2.6.6:

$$Entry\,mach = \frac{Mach_{max} * (\rho_{local,oxidizer} * |v| * A_t)}{(\rho_{local,total} * (0.000000000001 + |v_{max}|) * A_t)} \qquad (57)$$

where:

$Mach_{max}$ is the maximum fuel entry Mach value defined by the programmer,
$\rho_{local,\ oxidizer}$ is the oxidizer density in the control volume below the solid fuel surface,
0.000000000001 value is simply used as a programming solution to prevent fatal errors for control volumes with no velocity field.

This formula is established taking into consideration the influence of oxidizer flow on the regression rate [11]. It can be calibrated using experimental data.

3.1.2.2 Rate of reaction

At each control volume and per each time-step, equation (12) is applied to calculate the rates of elements' change considering equation (11), here repeated for convenience:

$$N_2O + C_2H_4 + (5/2)\ O_2 \longrightarrow 2\ N + 2\ H_20 + 2\ C0_2 \qquad (11)$$

3.1.3 **Thrust curves**

The total thrust provided by the engine, at each time-step is given by equation (1), here repeated for convenience:

$$F = \dot{m} * v_e - (P_e - P_a) * A_e \qquad (1)$$

where $\dot{m}$ is the average mass flow from the last gas control volumes near the chamber exit.

v_e is calculated for two distinct situations:

1. with De Laval nozzle (ideal nozzle conditions and with P_e equal to P_a)
2. without nozzle

For the first situation, equation (9) is used to calculate v_e. For situation two, the average velocity of the last gas control volumes near the chamber exit is calculated and v_e is considered to have that value. For both cases, all required gas properties are considered the average values of the last gas cells near the chamber's exit.

3.2 Software Engineering Process

3.2.1 **Programming language**

The main programming language used in the development of the numerical simulator for hybrid rocket engines (Hybrid Engine Simulation Software – HESS) was *J2SE* (*JAVA 2 Standard Edition*).

Software was developed as a stand-alone application in order to write data to text files (option not available for Applets).

There are three main reasons why JAVA was chosen:

1. Platform-independent programming language
2. Object-orientated
3. Programming language in which the author has extensive knowledge

HESS being platform independent is essential for future uses in commercial and/or educational studies. The main purpose of numerical simulations is cost- and time-saving, it would be illogical to have additional costs associated with acquiring expensive specific OS or requiring additional time for porting *.

JAVA is an object-orientated programming language. This feature helps reduce the complexity and redundancy of the code and thus saves time in development phase, debuging, and reduces the probability of existence of errors.

Being the author's most trusted programming platform had obvious time-saving benefits during the development phase.

Although JAVA is known for being slower than the usual programming languages chosen for aerospace applications (C, C++, ADA), this is not a critical factor in this case since the simulator is not real-time dependent.

* - Source code modifications to make software compatible with different platforms and/or operating systems.

3.2.2 **Software architecture**

3.2.2.1 Scheme

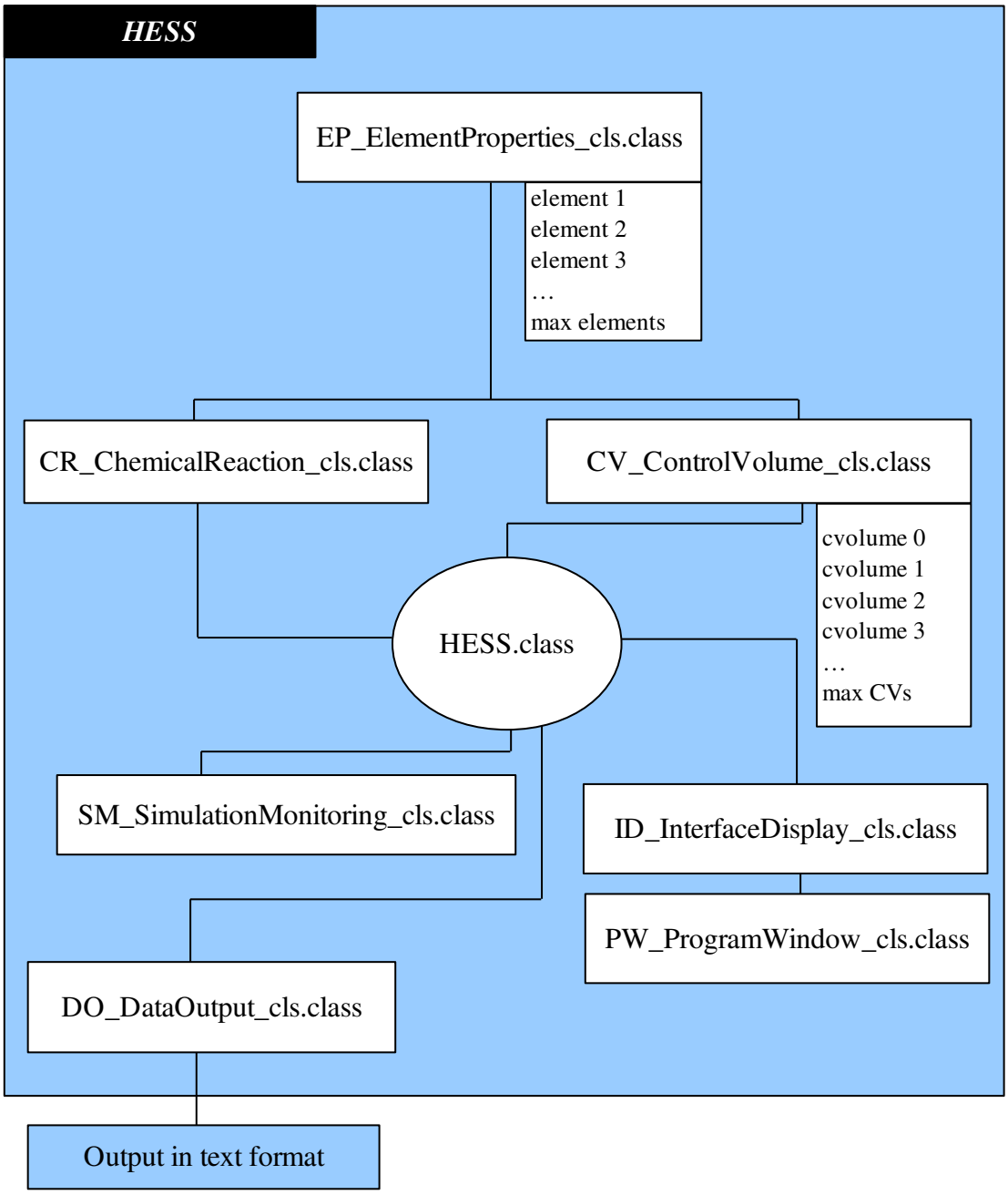

3.2.2.2 Description of JAVA segment classes

- *HESS.class* is the main class of the JAVA segment. Here all the other classes are interlinked.

- *EP_ElementProperties_cls.class* stores element specific values for each of the chemical elements existing in the combustion chamber. A number of objects equal to the number of existing elements is constructed.

- *CV_ControlVolume_cls.class* is responsible for most the calculations involved with a single control volume. This is where Euler equations are computed for gaseous control volumes and also where artificial sublimation calculations are done for solid fuel control volumes.

- *CR_ChemicalReaction_cls.class* applies the Arrhenius equations for each individual gaseous control volume thus calculating the rates of chemical elements' change.

- *SM_SimulationMonitoring_cls.class* makes a series of calculations' checks at each time-step to ensure that the physical laws and basic thermodynamic considerations aren't violated. The mass conservation law and CFL are two of the checks performed. Other checks related with temperature, pressure and energy are also done. If some of these critical checks is violated, the program logs the event and automatically shuts-down.

- *ID_InterfaceDisplay_cls* and *PW_ProgramDisplay_cls* are classes purely related with the function of graphical display and maintaining the program cycle.

- *DO_DataOutput_cls.class* writes relevant data into various distinct text files.

3.2.2.3 PDL

Program Design Language is a method of describing a program's code sequence using plain words.

HESS repeats the following sequence for each time-step though the simulation's duration:

1) Creation of control volumes' grid from rocket engine geometry

2) Define initial conditions

3) For each control volume: calculate ρ, ρu, ρv, ρw and ρe variations

- Update entry oxidizer and fuel mass as well as exiting mass information

4) Redefine initial conditions

- update velocity
- update density
- update mass portions
- update mass
- update total energy
- apply slip condition
- update temperature
- update enthalpy
- update gas individual constant
- update local Mach number
- update pressure
- set new conserved quantities for next iteration

5) Calculate rates of reaction

6) Modify mass information for control volumes where reactions occurred

7) Update mass fraction information

8) Run Simulation Monitoring class functions to verify data integrity

9) Display data

10) Repeat from step 2) until simulation time ends

3.3 Testing and Validation

Testing and validation of the mathematical method used in the simulator is done through two steps:

1. Ensuring equations do not diverge and basic physics' laws and considerations are not violated
2. Analysing initial results comparing them with actual rocket prototype test-fire results and conclusions from literature.

Although theoretical results are not expected to be precisely approximate to the practical results, they should be proportionally similar.

Chapter IV

4.1 Study Case

H2, Aspire-Space's small scale hybrid rocket engine geometry was used as test example during software development.

Figure 8 shows H2 basic geometry.

Range of testing oxidizer input Mach number was between 0.3 and 0.6.

4.2 Theoretical Results

The following graphics represent the combustion chamber of the H2 rocket. Although the geometry represented isn't equal to the one of figure 8, the geometry parameters computed by HESS are those previously indicated.

Purple stripe represents the grain length location. Far left vertical blue stripe represents the fuel injector while far right vertical green stripe is the gas chamber exit.

The actual dimensions of inlet and outlet control volumes are much smaller than the rest. Dimensions of control volumes of the pos-combustion chamber are the largest.

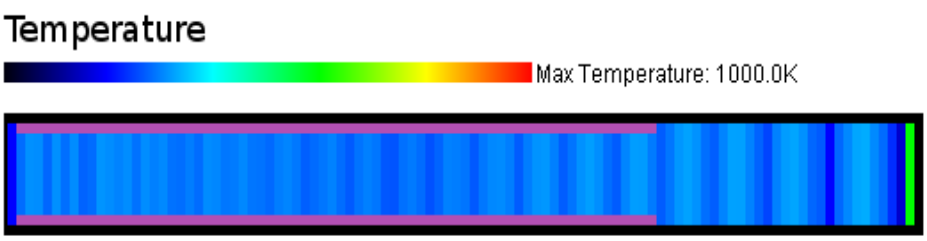

Fig. 13 – Temperature gradient in initial phase of oxidizer injection.

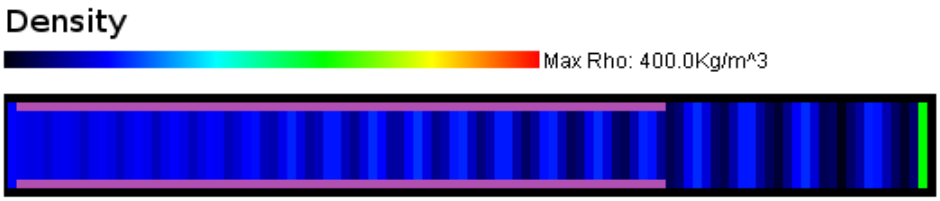

Fig. 14 – Density gradient in initial phase of oxidizer injection.

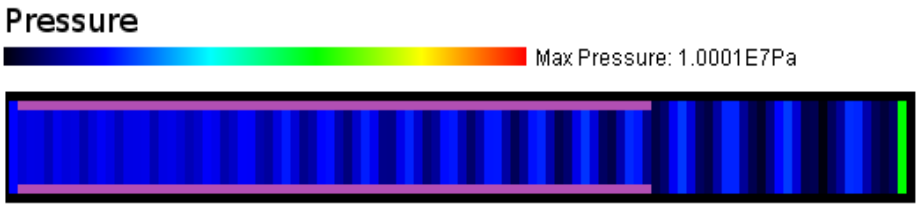

Fig. 15 – Pressure gradient in initial phase of oxidizer injection.

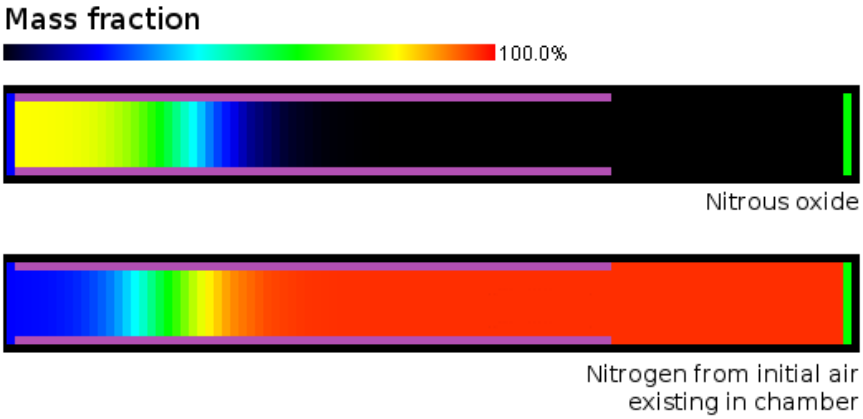

Fig. 16 – Mass fraction gradient in initial phase of oxidizer injection.

4.3 Observations

The following software functions worked successfully using current Mathematical method:

- Flow calculation for oxidizer:
    1. Temperature gradient prediction
    2. Density gradient prediction
    3. Gas velocity gradient prediction
    4. Pressure gradient prediction
    5. Local mass portions prediction

- Regression rate prediction

As expected, oxidizer temperature and pressure have greater order values near the injector and near the nozzle throat. The opposite happens with velocity.

As can be observed from oxidizer mass portion and air mass fraction (80% N_2), without the use of artificial dissipation, mass fractions calculations are correctly synchronized with the flow solver.

Discontinuities in flow calculations can be observed.

Stiffness related problems with flow solver currently prevents some implemented software functions of correctly working:

- 3D flow calculation
- Adding HPDE to main gas flow which also prevents calculating reaction products and thrust curves

So far, attempts of activating these options result in divergent results.

Chapter V

5.1 Future Work

For actual use of this kind of software, extensive testing is required in future studies.

Tests will consist in applying HESS to various propellant configurations in order to calibrate the software to present theoretical results that are approximate to the real performance of rocket engines.

The three-dimensional simulation should be once again attempted with a new set of boundary conditions.

Artificial dissipation function should be synchronized with mass fraction calculations in order to allow fuel (in gaseous state) entry and maintain currently working features.

Grid geometry related calculations of the Euler solver can be upgraded, thus providing a smoother, more accurate transition between cells. This would reduce flow discontinuities and therefore reduce errors.

Optionally, the flow solver can be extended to determine sonic and supersonic flows. This new feature would allow the solver to be extended to nozzle calculations thus ending the need to calculate engine thrust apart with equation (9).

Reaction process solver should be extended to be more accurate. Two-step chemistry models present better results than one-step models [11] and thus this model should be implemented as well.

Due to lack of time, an user interface wasn't developed and most of initial data input is hard-coded. In future work, HESS should feature a Swing based interface for data input.

5.2 Conclusion

Rocket engine simulation software was partially developed (alpha version) and first test simulations were performed.

As expected, initial results weren't sufficiently approximate to practical data obtained from the actual engine test-fire.

However simulation results show that relations between various parameters involved in engine performance are valid.

Unlike what was initially intended by the Author, not all hybrid rocket fuel geometries can be simulated. This happens because of strict flow solver limitations caused by boundary conditions.

Because of flow solver restrictions in building the grid, the actual gas flow of pre-combustion and pos-combustion chamber sections can not be exactly described by this methodology.

For currently implemented features, when calibrated, HESS has the potential to present better regression rate predictions for each of the solid fuel surface points than the ones obtained with equation (10), since it uses the flow information from the immediate control volume near that specific point location. This also allows HESS to determine regression rates for many non-cylindrical solid fuel geometries, which equation (10) cannot.

Although a purely theoretical use of this type of software can't determine approximate real engine performance results, calibrating the simulator with practical data from various propellant combinations will result in improved predictions.

The use of software simulations provides sufficiently good insight into rocket engines' performance.

Simulations are faster and cheaper than actual engine prototype testing, thus being capable to significantly reduce development costs and time.

If HESS is calibrated for a given propellant combination, various engine performance simulations can be obtained in one to three days' work.

This however, does not mean engine prototype testing can be neglected! Actual engine test-fire is still crucial and their results far more significant than computer simulations. Software simulations

simply allow engineers to quickly reduce the number of possible engine configurations during development phase.

Reduction of costs associated with space access is necessarily linked with the reduction of development time and costs of spacecraft and/or spacecraft related operations. Software plays a major role in this field since it is capable of significantly reducing the need of expensive specialized human resources by automatically performing predefined tasks much quicker.

References

Books:

[1] G. Sutton, O.Biblarz: “Rocket Propulsion Elements”, John Wiley & Sons, 7th Edition, 2001, United States of America.
[2] R. Fox, A. McDonald: “Introduction to Fluid Mechanics”, John Wiley & Sons, 4th Edition, 1994, United States of America.
[3] C. Laney: “Computational Gasdynamics”: Cambridge University Press, 1998, United States of America
[4] R. Löhner: Applied CFD Techniques, John Wiley & Sons, 2nd Edition, 2008, United States of America
[5] K. Kuo: “Principles of Combustion”, John Wiley & Sons, 1986, Singapore
[6] I. Glassman: “Combustion”, Academic Press, 1977, United States of America.
[7] J. London III: "LEO On the Cheap - Methods for Achieving Drastic Reductions in Space Launch Costs”, 1994, United States of America.
[8] M. Lobo: “Time-Marching – A step-by-step guide to flow solver”, Ashgate Publishing Company, 1997, Unites States of America
[9] C. Fletcher: “Computational Techniques for Fluid Dynamics – Volume I”, Springer-Verlag, 2nd Edition, Germany
[10] C. Fletcher: “Computational Techniques for Fluid Dynamics – Volume II”, Springer-Verlag, 2nd Edition, Germany

Papers:

[11] Guobio C., Hui T.: “Numerical Simulation of the Operation Process of a Hybrid Rocket Motor”, American Institute of Aeronautics and Astronautics, 2006
[12] L. Smoot, C. Price: “Pressure Dependence of Hybrid Fuel Regression Rates”, American Institute of Aeronautics and Astronautics, 1967
[13] L. Smoot, C. Price: “Regression Rates of Metalized Hybrid Fuel Systems”, American Institute of Aeronautics and Astronautics, 1965
[14] L. Smoot, C. Price: “Regression Rates of Non-Metalized Hybrid Fuel Systems”, American Institute of Aeronautics and Astronautics, 1965
[15] J. Majdalani, A. Vyas, G. Flandro: “Higher Mean-Flow Approximation for Solid Rocket Motors with Radially Regressing Walls”, American Institute of Aeronautics and Astronautics, 2002

[16] R. Newlands: “AspireSpace Technical Series”, http://www.aspirespace.org.uk, 13th May 2007 update, available as of 1st January 2009.

Websites:

[17] R. Brauning: “Rocket and Space Technology”, http://www.braeunig.us/space/index.htm, available as of 1st January 2009.
[18] Engineering Toolbox: http://engineeringtoolbox.com, available as of 1st January 2009.
[19] GRI-Mech Homepage: http://www.me.berkeley.edu/gri_mech, available as of 29th June 2009.
[20] Aspire-Space Homepage: http://www.aspirespace.org.uk, available as of 11th November 2008.